molecular pharmaceutics

articles

Lactoferrin-Conjugated Biodegradable Polymersome Holding Doxorubicin and Tetrandrine for Chemotherapy of Glioma Rats

Zhiqing Pang,[†] Liang Feng,[†] Rongrong Hua,[‡] Jun Chen,[†] Huile Gao,[†] Shuaiqi Pan,[†] Xinguo Jiang,*[,†] and Peng Zhang[‡]

School of Pharmacy, Fudan University, Shanghai, P. R. China, 201203

Received August 20, 2010; Revised Manuscript Received October 14, 2010; Accepted October 19, 2010

Abstract: The blood-brain barrier (BBB) and multidrug resistance (MDR) are the main causes for poor prognosis of glioma patients after chemotherapy. To explore the way for settling this problem, in this study, a novel antitumor agent loaded drug delivery system, lactoferrin-conjugated biodegradable polymersome holding doxorubicin and tetrandrine (Lf-PO-Dox/Tet), integrating both BBB and glioma-targeting moiety and MDR inhibitor, was designed and its chemotherapy for glioma rats was evaluated. Biodegradable polymersome (PO) encapsulating both doxorubicin (Dox) and tetrandrine (Tet) was prepared by the thin-film hydration method (PO-Dox/Tet) and then conjugated with lactoferrin (Lf) to yield Lf-PO-Dox/Tet with an average diameter around 220 nm and surface Lf molecule number per polymersome around 40. Compared with PO-DOX, PO-Dox/Tet, and Lf-PO-Dox, Lf-PO-Dox/Tet demonstrated the strongest cytotoxicity against C6 glioma cells and the greatest uptake index by C6 cells. In vivo imaging analysis indicated that Lf-PO labeled with a near-infrared dye could enter the brain and accumulate at the tumor site. Pharmacokinetics and tissue distribution results also showed that Lf-PO-Dox/Tet accumulated more in the right hemisphere than other groups of polymersomes. Pharmacodynamics results revealed that tumor volume of the Lf-PO-Dox/Tet group was significantly smaller than that of other therapeutic groups, and the median survival time of Lf-PO-Dox/Tet group was longer than that of Lf-PO-Dox group and significantly longer than those of the other three therapeutic groups. These results suggested that Lf-PO-Dox/Tet could have therapeutic potential for gliomas.

Keywords: Lactoferrin; biodegradable polymersome; doxorubicin; tetrandrine; chemotherapy; glioma

Introduction

As the most common intracranial malignant tumor, gliomas account for more than 40% of incidence of primary brain tumors.[1] Treatments for gliomas usually involve combined therapies of surgery, radiotherapy and chemotherapy, depending on the location and degree of malignancy.[2] However, the infiltration to normal surrounding brain parenchyma made it impossible to thoroughly eradicate gliomas using surgery, resulting in inevitable relapse.[3] On the other hand, chemotherapeutic drugs could hardly reach brain tumor cells but with systemic side effects just like those of radiotherapy. All these contributed to the poor effectiveness of treatment regimens for gliomas.

* To whom correspondence should be addressed. Mailing address: 617 Research Building, 826 Zhangheng Road, Shanghai, P. R. China, 201203. Telephone: 86-21-51980067. E-mail: xgjiang@shmu.edu.cn.

[†] Department of Pharmaceutics.

[‡] Department of Pharmacology.

(1) Colman, H.; Aldape, K. Molecular predictors in glioblastoma. *Arch. Neurol.* **2008**, *65* (7), 877–883.

(2) Lu, C.; Shervington, A. Chemoresistance in gliomas. *Mol. Cell. Biochem.* **2008**, *312*, 71–78.

(3) Silbergeld, D. L.; Chicoine, M. R. Isolation and characterization of human malignant glioma cells from histologically normal brain. *J. Neurosug.* **1997**, *86* (3), 525–531.

10.1021/mp100277h © **2010 American Chemical Society**
Published on Web 10/19/2010

Multidrug resistance (MDR) presents one of the main obstacles for chemotherapeutic drugs to gain access into brain tumor cells effectively. Among the quite a few mechanisms of MDR, exocytosis mediated by translocator of ATP-binding cassette (ABC) superfamily was most commonly seen, including P-glycoprotein (P-gp), multidrug resistance-associated protein (MRP), breast cancer resistance protein (BCRP), and so forth. P-gp and BCRP are overexpressed in glioma cells and glioma blood vessels, rigidly restricting the entry of antitumor drugs.[3] The blood-brain barrier (BBB) presents another main hindrance for chemotherapeutic drugs.[4,5] The unique anatomical structure together with an overexpression of MRP and P-gp in astrocytes and brain capillary endothelial cells (BCECs), respectively, consolidates the barrier function of the BBB,[6] hindering the chemotherapy of the active glioma cells infiltrated to normal surrounding brain parenchyma where the BBB remains intact, and allowing progression of the tumor at these sites. Moreover, poor site-specific distribution to glioma tissue and serious systemic toxicities of most antitumor agents also make up the main obstacles of effective tumor chemotherapy.

Lactoferrin (Lf) is a novel brain targeting ligand that has emerged in recent years, and several studies reported that drug-loaded carriers were able to transport across the BBB by mediation of Lf with high efficiency superior to transferrin.[7,8] Our lab also adopted Lf as a brain targeting ligand which was conjugated with PEG-PLA nanoparticles, achieving improved uptake by the BBB model cells and increased drug delivery to mouse brain.[9] What is more important is that low-density lipoprotein receptor-related protein (LRP), the receptor of Lf,[10] was proved overexpressed in glioma cells[11,12] and mediated the transcytosis of multiple ligands across the BBB such as Lf,[13] melanotransferrin,[14] receptor associated protein,[15] and Angiopep-2 peptide.[16] Therefore, as a both BBB and glioma targeting ligand, Lf has great potential to overcome the BBB and target drug carriers to brain tumors, increasing the specific interaction of carriers with glioma cells and enhancing the amount of drug delivered into these cells after tumorous accumulation of carriers. To date, no reports have been published about the application of lactoferrin in glioma targeting.

As a new class of synthetic thin shelled capsules based on block copolymer chemistry, polymersomes are self-assembled vesicles of amphiphilic block copolymers with thicker and tougher membranes than those of lipids,[17,18] resulting in higher stability compared to liposomes. The combination of a thick wall for a hydrophobic drug and a vesicular lumen for a hydrophilic drug will lead to synergistic effects such as cocktails. Moreover, the physical and chemical properties of polymersomes including particle size, drug loading, surface modification, and even in vivo behavior may be broadly tunable through a rich diversity of block copolymer chemistries.[19] Therefore, polymersomes are good candidates for drug delivery systems (DDS) which are currently being developed by many groups.[20]

Tetrandrine (Tet), one of the bisbenzylisoquinoline alkaloids, has been used as an antifibrotic drug to treat lesions of silicosis in China since the 1960s. Tet was a potent MDR inhibitor which was proved by enhanced efficacy of doxo-

(4) Juillerat, J. L. The targeted delivery of cancer drugs across the blood-brain barrier: chemical modifications of drugs or drug-nanoparticles. *Drug Discovery Today* **2008**, *13*, 1099–1106.

(5) Marc, C. C. Anticancer therapies and CNS relapse: overcoming blood−brain and blood−cerebrospinal fluid barrier impermeability. *Expert Rev. Neurother.* **2010**, *10* (4), 547–561.

(6) Oh, K. T.; Baik, H. J.; Lee, A. H.; Oh, Y. T.; Youn, Y. S.; Lee, E. S. The reversal of drug-resistance in tumors using a drug-carrying nanoparticular system. *Int. J. Mol. Sci.* **2009**, *10*, 3776–3792.

(7) Ji, B.; Maeda, J.; Higuchi, M. Pharmacokinetics and brain uptake of lactoferrin in rat. *Life Sci.* **2006**, *78* (8), 851–855.

(8) Huang, R. Q.; Ke, W. L.; Liu, Y.; Jiang, C.; Pei, Y. Y. The use of lactoferrin as a ligand for targeting the polyamidoamine-based gene delivery system to the brain. *Biomaterials* **2008**, *29*, 238–246.

(9) Hu, K. L.; Li, J. W.; Shen, Y. H.; Lu, W.; Gao, X. L.; Zhang, Q. Z.; Jiang, X. G. Lactoferrin-conjugated PEG-PLA nanoparticles with improve brain delivery: *in vivo* and *in vitro* evaluations. *J. Controlled Release* **2009**, *134*, 55–61.

(10) Suzuki, Y. A.; Lopez, V.; Lonnerdal, B. Mammalian lactoferrin receptors: structure and function. *Cell. Mol. Life Sci.* **2005**, *62* (22), 2560–2575.

(11) Maletinska, L.; Blakely, E. A.; Bjornstad, K. A. Human glioblastoma cell lines: levels of low-density lipoprotein receptor and low density lipoprotein receptor-related protein. *Cancer Res.* **2000**, *60*, 2300–2303.

(12) Uden, E. V.; Carlson, G.; Hyslop, P. Abberrant presenilin-1 expression downregulates LDL receptor-related protein (LRP): Is LRP central to Alzheimer's Disease pathogenesis. *Mol. Cell. Neurosci.* **1999**, *14*, 129–140.

(13) Fillebeen, C.; Descamps, L.; Dehouck, M. P. Receptor-mediated transcytosis of lactoferrin through the blood-brain barrier. *J. Biol. Chem.* **1999**, *274* (11), 7011–7017.

(14) Demeule, M.; Poirier, J.; Jodoin, J.; Bertrand, Y.; Desrosiers, R. R.; Dagenais, C.; Nguyen, T.; Lanthier, J.; Gabathuler, R.; Kennard, M.; Jefferies, W. A.; Karkan, D.; Tsai, S.; Fenart, L.; Cecchelli, R.; Beliveau, R. High transcytosis of melanotransferrin (p97) across the blood−brain barrier. *J. Neurochem.* **2002**, *83*, 924–933.

(15) Pan, W.; Kastin, A. J.; Zankel, T. C.; van Kerkhof, P.; Terasaki, T.; Bu, G. Efficient transfer of receptor-associated protein (RAP) across the blood−brain barrier. *J. Cell Sci.* **2004**, *117*, 5071–5078.

(16) Demeule, M.; Currie, J. C.; Bertrand, Y.; Che, C.; Nguyen, T.; Regina, A.; Gabathuler, R.; Castaigne, J. P.; Beliveau, R. Involvement of the low-density lipoprotein receptor-related protein in the transcytosis of the brain delivery vector Angiopep-2. *J. Neurochem.* **2008**, *106*, 1534–1544.

(17) Discher, D. E.; Eisenberg, A. Polymer vesicles. *Science* **2002**, *297*, 967–973.

(18) Discher, D. E.; Ahmed, F. Polymersomes. *Annu. Rev. Biomed. Eng.* **2006**, *8*, 323–41.

(19) Pang, Z. Q.; Lu, W.; Gao, H. L.; Hu, K. L.; Chen, J.; Zhang, Q. Z.; Gao, X. L.; Jiang, X. G.; Zhu, C. Q. Preparation and brain delivery property of biodegradable polymersomes conjugated with OX26. *J. Controlled Release* **2008**, *128*, 120–127.

(20) Discher, D. E.; Ortiz, V.; Srinivas, G.; Klein, M. L.; Kim, Y.; Christian, D.; Cai, S.; Photos, P.; Ahmed, F. Emerging applications of polymersomes in delivery: from molecular dynamics to shrinkage of tumors. *Prog. Polym. Sci.* **2007**, *32*, 838–857.

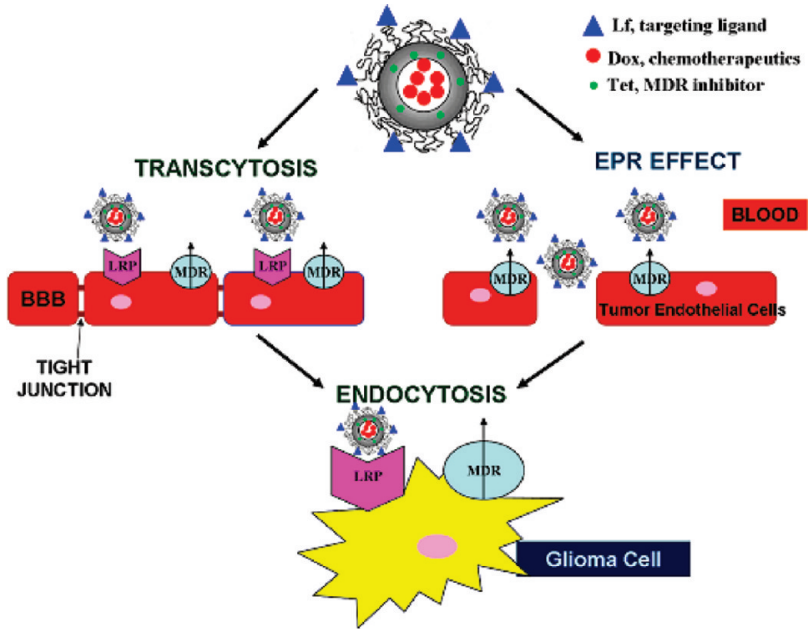

Figure 1. Design of lactoferrin-conjugated biodegradable polymersome for glioma targeting.

rubicin both in vitro and in nude mice bearing tumors,[21,22] making it a good choice to be incorporated in biodegradable polymersomes for MDR reversing just like verapamil loaded in liposomes[23] and ceramide encapsulated in nanoparticles.[24]

On the basis of the above considerations, a novel nanoscaled drug delivery system was designed employing biodegradable polymersomes as carriers simultaneously holding doxorubicin (Dox) as a model antitumor drug and tetrandrine (Tet) as an MDR inhibitor (Figure 1). On the surface of polymersomes, Lf was conjugated as glioma targeting ligand meanwhile with the ability to lead polymersomes to overcome the obstruction of the BBB. After accumulation of polymersomes in glioma was achieved by the EPR effect and overcoming BBB, the specific interaction of Lf-conjugated polymersomes with glioma cells was expected to enhance drug delivery into these cells, improving the chemotherapy of glioma. Targeted delivery to glioma of the Lf-conjugated polymersomes labeled with near-infrared dye was first examined in glioma model rats. In vitro drug delivery characteristics toward C6 glioma cells and in vivo pharmacokinetics together with tissue distribution and pharmacodynamics of the Lf-conjugated polymersomes holding Dox and Tet were investigated subsequently.

Materials and Methods

Materials and Animals. Methoxy poly(ethylene glycol)−poly(ε-caprolactone) (MPEG3k-PCL15k) and α-carboxyl poly(ethylene glycol)−poly(ε-caprolactone) (HOOC-PEG3.4k-PCL15k) were synthesized as previously described.[19] Lactoferrin from bovine colostrum (Lf), 1-dimethylaminopropyl-ethylcarbodiimide hydrochloride (EDC), *N*-hydroxysuccinimide (NHS), and 3-(4,5-dimethylthiazol-2-yl)-2,5-diphenyltetrazolium bromide (MTT) were purchased from Sigma-Aldrich (Saint Louis, MO). 1,1′-Dioctadecyl-3,3,3′,3′-tetramethylindotricarbocyanine Iodide (DiR), a near-infrared dye, was offered by Biotium (Hayward, CA). Bovine lactoferrin ELISA quantification kit was ordered from Bethyl (Montgomery, TX). BCA protein assay kit was ordered from Shenergy Biocolor Bioscience and Technology Co., Ltd. (Shanghai, China). Doxorubicin (Dox) and tetrandrine (Tet) were purchased from Beijing Huafeng United Technology (China) and National Institute for the Control of Pharmaceutical and Biological Products (China), respectively. C6 glioma cell line from rat was obtained from the American Type Culture Collection. Fetal bovine serum (FBS) and related cell culture medium were purchased from Invitrogen (Gibco, Carlsbad, CA). Plastic cell culture dishes, plates, and flasks were ordered from Corning Incorporation (Lowell, MA). Double distilled water was purified using a Millipore Simplicity System (Bedford, MA). All other chemicals were of analytical grade and used without further purification.

Sprague-Dawley rats (weighing 180−220 g) were provided by Super-B&K Laboratory Animal Corp. Ltd. (Shanghai, China). The animals involved in this study were treated

(21) Fu, L. W.; Liang, Y. J.; Deng, L. W.; Ding, Y.; Chen, L. M.; Ye, Y. L.; Yang, X. P.; Pan, Q. C. Characterization of tetrandrine, a potent inhibitor of P-glycoprotein-mediated multidrug resistance. *Cancer Chemother. Pharmacol.* **2004**, *53*, 349–356.
(22) Fu, L. W.; Zhang, Y. M.; Liang, Y. J.; Yang, X. P.; Pan, Q. C. The multidrug resistance of tumour cells was reversed by tetrandrine *in vitro* and in xenografts derived from human breast adenocarcinoma MCF-7/adr cells. *Eur. J. Cancer* **2002**, *38*, 418–426.
(23) Wang, J. C.; Liu, X. Y.; Lü, W. L.; Lee, H. S.; Goh, B. C.; Zhang, Q. The *in vitro* cytotoxicity and *in vivo* toxicity of doxorubicin antiresistant stealth liposomes. *Acta Pharm. Sin.* **2005**, *40* (5), 475–480.
(24) Van, V. L. E.; Duan, Z.; Seiden, M. V. Modulation of intracellular ceramide using polymeric nanoparticles to overcome multidrug resistance in cancer. *Cancer Res.* **2007**, *67*, 4348–4850.

according to protocols evaluated and approved by the ethical committee of Fudan University.

Preparation of DiR-Loaded Polymersomes. The thin-film hydration method as described previously[25] was employed to prepare DiR-loaded polymersomes. Concisely, 50.0 mg of MPEG3k-PCL15k, 2.5 mg of HOOC-PEG3.4k-PCL15k, and 1 mg of DiR were dissolved in 20 mL of dichloromethane, which was evaporated under vacuum at 25 °C in a rotary evaporator, leading to the formation of a polymeric film onto the vial wall. This film was then fully hydrated in 20 mL of phosphate buffer (PB, 0.1 M, pH 6.0) by fiercely shaking at 65 °C for 30 min. The obtained vesicle dispersion was extruded through a 0.45 μm filter membrane (Millex-HV, Millipore) to remove the copolymer aggregates and to narrow the vesicle size distribution. By means of ultrafiltration, free DiR was removed and the vesicle dispersion was concentrated to yield DiR-loaded polymersome (PO-DiR). For Lf conjugation, solid EDC (20 mg) and NHS (50 mg) were then added into the PO-DiR dispersion to activate surface carboxyl groups on polymersomes by stirring at room temperature for 20 min. After unreacted EDC and NHS were removed and the buffer was exchanged with phosphate buffered saline (PBS, 0.01 M, pH 7.4) by ultrafiltration, 1.0 mg of Lf was added into the obtained vesicle dispersion and stirred for 3 h. By means of ultrafiltration again, unconjugated protein was removed and the vesicle dispersion was concentrated to yield Lf-conjugated DiR-loaded polymersome (Lf-PO-DiR). All operations were conducted away from light.

Preparation of Dox-Loaded Polymersomes. Blank polymersome was first prepared in the same way as described above except that DiR was eliminated and the hydration solution was changed to citrate buffer (0.2 M, pH 4.0). After hydration and filtration, the pH of the vesicle dispersion was neutralized to 7.4 by Na_2CO_3 (1 M), and 1 mL of Dox solution (2 mg/mL) was added and stirred in dark at room temperature for 24 h. By means of ultrafiltration, unencapsulated Dox was eluted and the vesicle dispersion was concentrated to yield Dox-loaded polymersome (PO-Dox). Thereafter, 0.5 mg of Tet dissolved in methanol was added into the PO-Dox dispersion and stirred for 6 h at room temperature, which was then subjected to dialysis against 100 mL of PBS at 4 °C for another 6 h to get rid of methanol and free Tet. By means of ultrafiltration again, the vesicle dispersion was concentrated to yield both Tet and Dox-loaded polymersome (PO-Dox/Tet). Lf was conjugated with PO-Dox and PO-Dox/Tet with the same procedure as described above.

Charaterization of Polymersomes. For morphological examination, blank polymersome in citrate buffer was concentrated and the buffer was exchanged with saline by means of ultrafiltration to avoid the reaction of uranyl ions with citrate ions during negative staining. After negative staining with 1% uranyl acetate solution, blank polymersome was observed via transmission electron microscopy (TEM; H-600, Hitachi, Japan). Vesicle size and zeta potential of polymersomes were determined by dynamic light scattering (DLS) analysis using a zeta potential/particle size analyzer (Nicomp 380ZLS) with a He−Ne laser at 632.8 nm. Drug loading capacity (DLC) and entrapment efficiency (EE) of DiR and Dox were determined by fluorescence spectrophotometry after dissolving polymersomes in acetonitrile. The average number of Lf molecules conjugated per polymersome was determined by using a lactoferrin ELISA kit and calculated by dividing the number of Lf molecules by the calculated average number of polymersomes using methods described by Oliver et al.[26]

In Vitro Cytotoxicity of Dox Loaded Polymersomes Against C6 Cells. C6 cells were seeded onto a 96-well plate at a density of 10^4 per well and incubated for 24 h before exposure to different Dox formulations with a series of concentrations for a further 24 h at 37 °C. Eight wells for untreated cells were prepared as controls. After exposure, the cytotoxicity of these formulations was assayed by the MTT method.[27] The experiments were performed in quadruplicate.

Cell Uptake and Intracellular Drug Distribution of Dox Loaded Polymersomes. A 24-well plate was seeded with C6 cells at a density of 10^5 per well, and the cells were allowed to attach for 24 h. Dispersions of PO-Dox, Lf-PO-Dox, PO-Dox/Tet, and Lf-PO-Dox/Tet as well as free Dox solution were each added into the medium in triplicate to make a final Dox concentration at 4 μg/mL in each well. After 4 h incubation at 37 °C, the medium was removed and the cells were stained with 1 μg/mL of 4′,6-Diamidino-2-phenylindole dihydrochloride (DAPI) for 10 min at room temperature. After PBS washing, the plate was subjected to observation under the fluorescence microscope (Olymus IX71, Japan).

Quantitative Determination of Cell Uptake of Dox Loaded Polymersomes. Similarly to the above, C6 cells were seeded onto 24-well plates at a density of 10^5 per well, and the cells were allowed to attach for 24 h. Four groups of polymersomes were respectively added into the medium to make a final Dox concentration at 4 μg/mL in each well (triplicate for each formulation). The plates were incubated for 1, 2, 4, 8, or 12 h at 37 °C. For each time point, cells in each well of the corresponding plate were washed three times with ice-cold PBS to remove surface-bound polymersomes and further incubated with 0.4 mL of 1% Triton X-100 overnight. Afterward, 25 μL of the cell lysate from each well was sampled to determine the total cell protein content using the BCA protein assay kit. The rest of the cell lysate was

(25) Photos, P. J.; Bacakova, L.; Discher, B.; Bates, F. S.; Discher, D. E. Polymer vesicles *in vivo*: correlations with PEG molecular weight. *J. Controlled Release* **2003**, *90*, 323–334.

(26) Olivier, J. C.; Huertas, R.; Lee, H. J.; Calon, F.; Pardridge, W. M. Synthesis of pegylated immunonanoparticles. *Pharm. Res.* **2002**, *19*, 1137–1143.

(27) Lu, W.; Tan, Y. Z.; Hu, K. L.; Jiang, X. G. Cationic albumin conjugated pegylated nanoparticle with its transcytosis ability and little toxicity against blood-brain barrier. *Int. J. Pharm.* **2005**, *295*, 247–260.

used for extraction and HPLC determination of Dox (Agilent 1200).[28] The uptake index (UI) was expressed as Dox (μg)/cellular protein (mg).

In Vivo Imaging of DiR-Loaded Polymersomes in Glioma Model Rats. The glioma model was established by stereotactically injecting C6 cells into the right striatum of rats.[29] The in vivo imaging system was applied to qualitatively investigate the brain delivery property of PO-DiR and Lf-PO-DiR in glioma model rats 10 days after transplantation. In brief, the model rat was anesthetized by intraperitoneal injection of 10% chloraldurate solution, and then its hair was shaved off all over the body. Later, it was placed in the dark chamber of the imaging system and the baseline was scanned to set up the detection threshold to make sure the background signal was avoided. The filters for excitation and emission were set at 730 and 790 nm, respectively. The rat was then i.v. injected with PO-DiR or Lf-PO-DiR at the dose of 0.5 mg/kg of DiR and subjected to fluorescence imaging which represented the in vivo distribution of polymersomes. After that, an X-ray image was collected for locating the fluorescence signal.

Pharmacokinetic and Tissue Distribution in Glioma Model Rats. Twelve days after C6 cell transplantation, 16 glioma model rats were randomly divided into four groups, which were treated with PO-Dox, Lf-PO-Dox, PO-Dox/Tet, and Lf-PO-Dox/Tet respectively via i.v. injection into the tail vein at a dose of 0.4 mg of Dox per rat. Blood samples were collected from the orbital plexus at 2, 5, 10, 20, 40, and 60 min after intravenous administration. Decapitation and heart perfusion with saline were conducted closely after the last blood sampling, and the brain tissue together with other organ samples were collected. Later, Dox concentration in plasma and tissue samples was measured by HPLC as previously described.[28] The pharmacokinetic parameters were calculated using the pharmacokinetic software DAS version 2.0.

Pharmacodynamic Experiments in Glioma Model Rats. Forty glioma model rats were equally and randomly divided into five groups, which were treated with saline, PO-Dox, Lf-PO-Dox, PO-Dox/Tet, and Lf-PO-Dox/Tet respectively via i.v. injection at 2, 5, 8, and 11 days after glioma transplantation, dosing at 1.5 mg/kg Dox. On the 7th day, half of the rats in each group were sacrificed, and so were the other half on the 14th day. Heart perfusion with 10% neutral buffered formalin was conducted after sacrifice, and the brain tissue sample was collected and fixed with 10% neutral buffered formalin for at least 48 h and then embedded in paraffin followed by routine hematoxylin and eosin (H&E) staining on 5 μm thick sections using routine protocols.[30] The maximum diameter (a) and minimum diameter (b) of glioma tissue was measured under stereomicroscope, and the tumor volume (V) in each animal was calculated as $V = 0.5ab^2$.

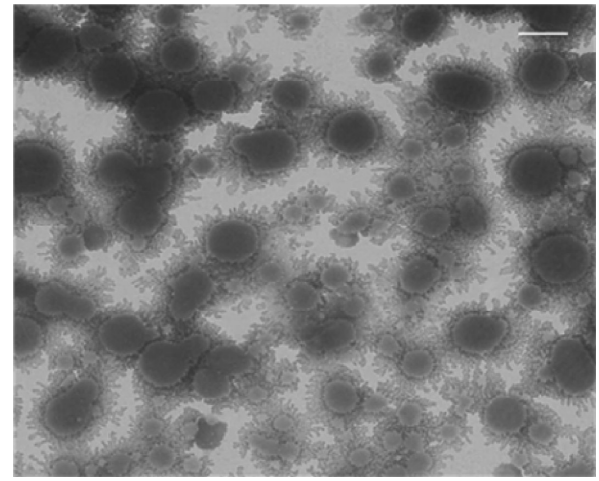

Figure 2. Transmission electron micrograph of blank polymersome. Bar = 200 nm.

Another 55 glioma model rats were subjected to the same grouping and therapeutic regimen as described above. Rat deaths of each group were recorded, and the corresponding survival curves were drawn.

Statistical Analysis. Statistical differences in uptake index, pharmacokinetic parameters, and tumor volume were determined by one-way analysis of variance (ANOVA), followed by post hoc analysis of Bonferroni for multigroup comparison. $P < 0.05$ was considered significant.

Results

Characterization of Polymersomes. It was found that a blend of MPEG-PCL(3k−15k) and COOH-PEG-PCL (3.4k−15k) spontaneously assembled into polymersomes, which was verified by TEM micrographs (Figure 2) in which vesicles were generally round with a diameter at around 200 nm. The well-defined thick membranes of polymersomes were obviously observed probably due to uranyl ions binding to surface carboxyl groups of polymersomes. A relative broad size distribution observed in TEM micrographs was proved by DLS analysis. The intensity-based vesicle size of PO-DiR and Lf-PO-DiR was 245.9 ± 45.0 and 248.4 ± 49.5 nm, respectively, indicating that Lf conjugation had no influence on the diameter of polymersomes. The same situation was observed for PO-Dox, Lf-PO-Dox, PO-Dox/Tet, and Lf-PO-Dox/Tet with nearly identical vesicle size at around 220 nm. Drug loading capacity of Dox in the four groups of polymersomes was about 4.4% with entrapment efficiency above 96%. Zeta potential of all the above-

(28) Pan, H.; Han, L. M.; Chen, W.; Yao, M.; Lu, W. Y. Targeting to tumor necrotic regions with biotinylated antibody and streptavidin modified liposomes. *J. Controlled Release* **2008**, *125*, 228–235.

(29) Lu, W.; Sun, Q.; Wan, J.; She, Z. J.; Jiang, X. G. Cationic albumin-conjugated pegylated nanoparticles allow gene delivery into brain tumors via intravenous administration. *Cancer Res.* **2006**, *66*, 11878–11887.

(30) Schoch, G.; Seeger, H.; Bogousslavsky, J.; Tolnay, M.; Janzer, R. C.; Aguzzi, A.; Glatzel, M. Analysis of prion strains by PrPSc profiling in sporadic Creutzfeldt-Jakob disease. *PLoS Med.* **2006**, *3*, e14.

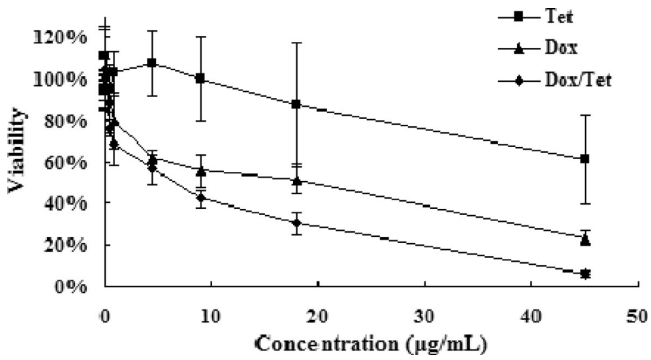

Figure 3. C6 viability−concentration curves for free Dox, Tet, or their blend.

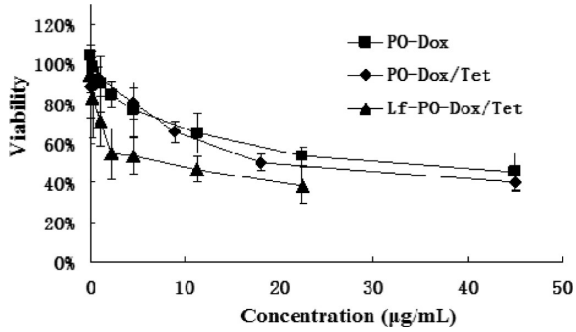

Figure 4. C6 viability−concentration curves for polymersomes.

mentioned polymersomes ranged from −10 to −9 mV, displaying similar stability with each other. The mean Lf molecule numbers per polymersome on the surface of Lf-PO-DiR, Lf-PO-Dox, and Lf-PO-Dox/Tet were 37 ± 2, 39 ± 2, and 40 ± 2, respectively, which were in a reasonable range for brain targeting justified in other studies.[8,9]

In Vitro Cytotoxicity Assay against C6 Cells. Cytotoxicity of free Dox, Tet, or a blend of the two drugs at a mass ratio of Dox/Tet = 4:1 against C6 cells was examined first. According to viability−concentration curves (Figure 3), the IC_{50} (drug concentration of 50% inhibition) of the blend and Dox alone was 6.4 and 20 μg/mL, respectively, showing that the cytotoxicity of the blend was 3.1 times higher than that of Dox alone. Meanwhile, the cytotoxicity of Tet alone was far lower than that of the other two formulations, suggesting that Tet greatly improved the cytotoxicity of Dox against C6 cells, but this improvement had little to do with the antitumor activity of Tet itself.

The cytotoxicity of Lf-PO-Dox/Tet, PO-Dox/Tet, and PO-Dox against C6 cells was investigated. Viability−concentration curves (Figure 4) showed that the IC_{50} (Dox concentration of 50% inhibition) of these three formulations was 8.4, 19.1, and 32.2 μg/mL, respectively, manifesting a 2.3 times intensification of cell inhibition of Lf-PO-Dox/Tet compared to PO-Dox/Tet, and 1.7 times intensification of cell inhibition of PO-Dox/Tet compared to PO-Dox, indicating a significant improved cytotoxicity mediated by Tet and Lf.

Cell Uptake and Intracellular Drug Distribution of Dox Loaded Polymersomes. Uptake of polymersomes into C6 cells was demonstrated by fluorescence microscopy photographs in which red fluorescence represented Dox and blue fluorescence referred to nuclei stained with DAPI (Figure 5). For free Dox, the red fluorescence nearly completely overlaid with the blue fluorescence, indicating that free Dox entered into the cells and mainly concentrated at the nucleus, where its cytotoxicity exerted. As regards Lf-PO-Dox/Tet, which acted as representative of Dox-loaded polymersomes since no difference could be qualitatively observed in the fluorescence microscopy photographs among them (data not shown), the red Dox fluorescence distributed mainly in the cytoplasm of cells except for partly in the nucleus, indicating that the cell uptake of Dox in free Dox group was mainly through diffusion mechanism, while the cell uptake of Dox in Lf-PO-Dox/Tet group was at least partially in a different way, possibly receptor-mediated endocytosis.

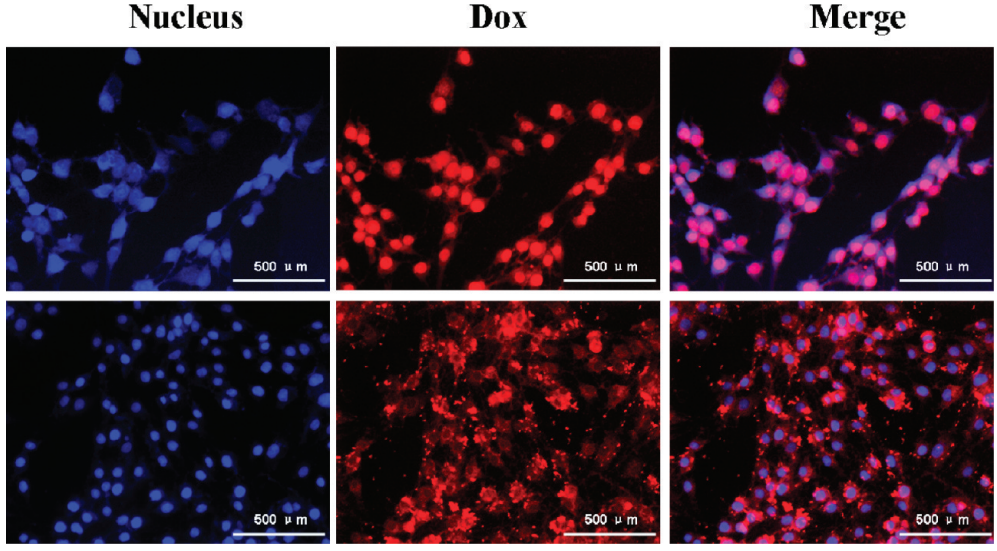

Figure 5. Fluorescence photographs of C6 cells after incubation for 4 h with polymersomes represented by Lf-PO-Dox/Tet (lower row) and free Dox (upper row).

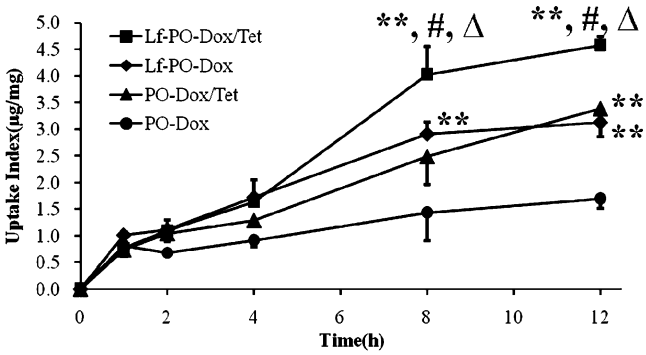

Figure 6. C6 uptake of different polymersomes at 37 °C for different incubation times (Dox concentration: 4 μg/mL). *$p < 0.05$, **$p < 0.01$ vs PO-Dox; #$p < 0.01$ vs PO-Dox/Tet; Δ $p < 0.01$ vs Lf-PO-Dox.

Quantitative Determination of Cell Uptake of Dox Loaded Polymersomes. Uptake of polymersomes by C6 cells increased with time (Figure 6). PO-Dox displayed relatively lower uptake, which increased by only 50% from 1 to 12 h. The other three groups exhibited similar uptake in the initial 4 h. However, 4 h later, uptake of Lf-PO-Dox/Tet was significantly higher than that of Lf-PO/Dox and PO-Dox/Tet. By 12 h, uptake of Lf-PO-Dox/Tet reached 1.5 times that of Lf-PO/Dox and PO-Dox/Tet and 3 times that of PO-Dox. These results proved that both Lf and Tet enhanced the cell uptake of Dox loaded polymersomes.

In Vivo Imaging of DiR-Loaded Polymersomes in Glioma Model Rats. With time elapsing, brain fluorescence intensity of the glioma model rat injected with Lf-PO-DiR gradually increased and this process sustained until 24 h (Figure 7, the upper row), which could be related with weakened body metabolism due to anesthesia and prolonged release behavior shaped by the polymersomes.[19] Moreover, the fluorescence region, especially the brightest site, leaned to the right of the brain, anterior to the ears and posterior to the epicanthus, which was in good accordance with the transplantation site of the right striatum, indicating that Lf-PO-DiR entered the brain and accumulated at the tumor site. On the contrary, the glioma model rat injected with PO-DiR did not exhibit an obvious intensifying process of brain fluorescence which just emerged at 4 h and retained low intensity at the tumor site all the time until 24 h (Figure 7, the lower row). According to the semiquantitative glioma fluorescence intensity−time curve (data not shown), the AUC_{0-t} of Lf-PO-DiR was 3.6 times higher than that of PO-DiR, confirming that Lf conjugation increased the glioma homing of Lf-PO-DiR.

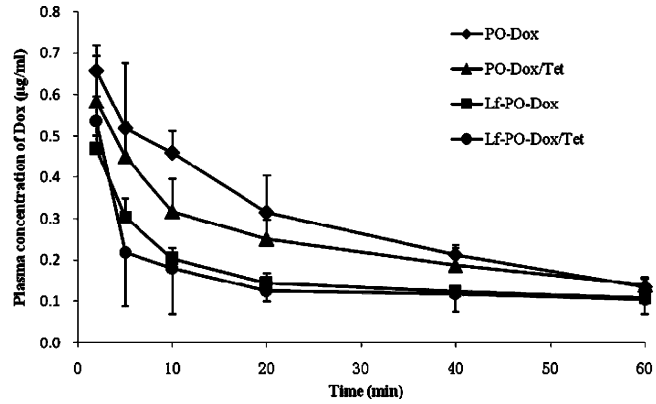

Figure 8. Concentration−time curves of doxorubicin in plasma after i.v. injection of polymersomes into glioma implanted rats ($n = 4$).

Pharmacokinetics Experiments in Glioma Model Rats. Plasma concentration−time curves of polymersomes after i.v. injection to glioma model rats were presented in Figure 8 with the corresponding pharmacokinetic parameters listed in Table 1. The descending curves revealed a gradual decreasing process of plasma Dox concentration, indicating polymersomes have long plasma circulation time after intravenous administration. According to the pharmacokinetic parameters, AUC_{0-t} of Lf-PO-Dox/Tet was significantly lower than that of PO-Dox/Tet, while $t_{1/2}$ of Lf-PO-Dox/Tet was slightly higher than PO-Dox/Tet. Similar relationship existed between Lf-PO-Dox and PO-Dox. There were no significant differences of the elimination rate constant (k) between groups and the MRT_{0-t} of all groups of polymersomes ranged from 21 to 28 h, suggesting Lf decoration and Tet loading had no significant influence on the long plasma circulation property of polymersomes.

Brain samples were separated into the left hemisphere and right hemisphere, and drug distribution in these two parts

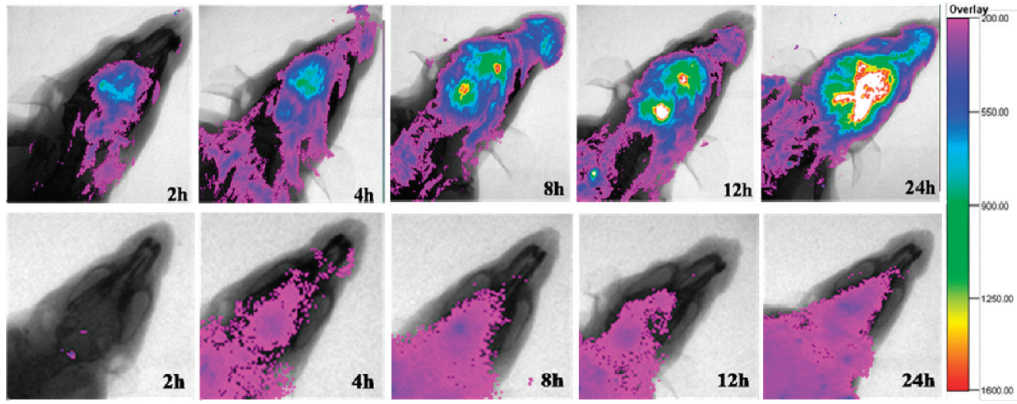

Figure 7. Brain fluorescence imaging of glioma model rats at a series of time points after i.v. injection of Lf-PO-DiR (the upper row) or PO-DiR (the lower row) at the dose of 0.5 mg/kg of DiR ($n = 4$).

Table 1. Pharmacokinetic Parameters of Doxorubicin in Plasma after i.v. Injection of Polymersomes into Glioma Implanted Rats[a]

PK parameter	PO-Dox	Lf-PO-Dox	PO-Dox/Tet	Lf-PO-Dox/Tet
AUC_{0-t} (μg/mL·min)	18.99 ± 2.86	10.45 ± 1.55[b]	14.69 ± 2.01	9.81 ± 4.28[b]
MRT_{0-t} (min)	21.41 ± 0.85	22.50 ± 0.91	22.72 ± 1.81	27.54 ± 3.75
k (min^{-1})	0.047 ± 0.002	0.044 ± 0.002	0.044 ± 0.004	0.037 ± 0.005
$t_{1/2}$ (min)	14.84 ± 0.59	15.60 ± 0.63	15.75 ± 1.26	19.09 ± 2.60

[a] Values were mean ± SD, $n = 4$. [b] $p < 0.05$ vs PO-Dox.

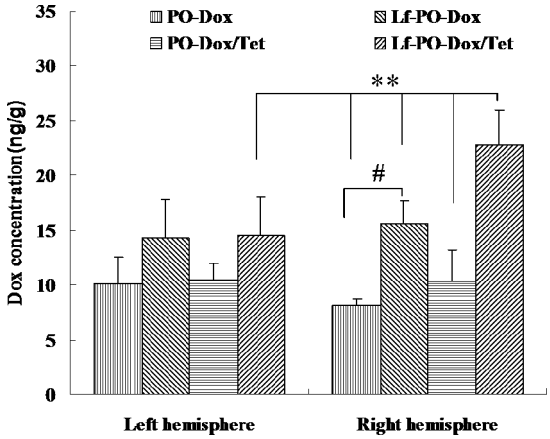

Figure 9. Brain distribution of Dox in the right and left hemisphere after i.v. injection of polymersomes ($n = 4$). Statistically significant difference by Student's t test when compared to the corresponding value of control. **$p < 0.01$ vs Lf-PO-Dox/Tet; #$p < 0.01$ PO-Dox vs Lf-PO-Dox.

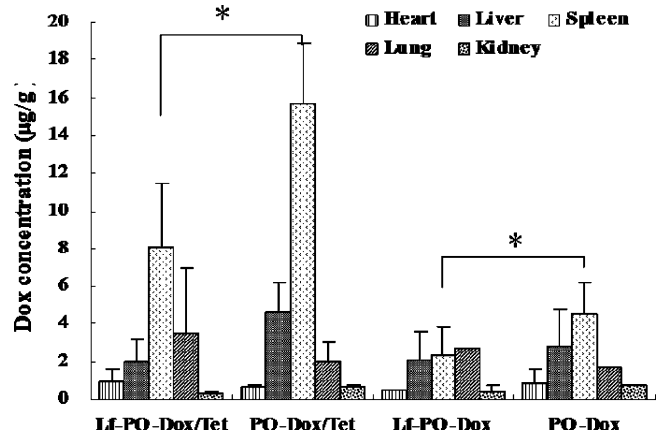

Figure 10. Distribution of Dox in heart, liver, spleen, lung, and kidney after i.v. injection of Dox-loaded polymersomes ($n = 4$). Statistically significant difference by Student's t test when compared to the corresponding value of control (*$p < 0.05$).

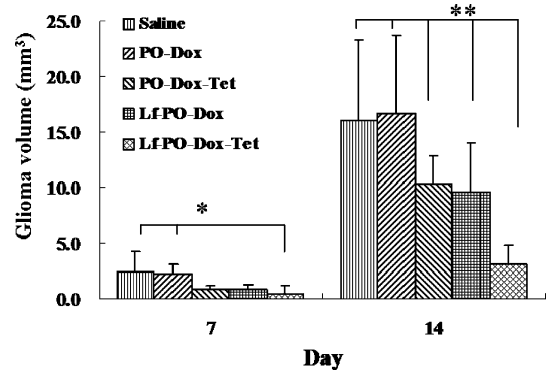

Figure 11. Glioma volume of different therapeutic groups at the 7th and 14th day ($n = 4$). *$p < 0.05$; ** $p < 0.01$ vs Lf-PO-Dox/Tet group.

was analyzed. The results (Figure 9) demonstrated that although glioma tissue was mixed with normal brain tissue in the right hemisphere, for the Lf-PO-Dox/Tet group, Dox concentration in the right hemisphere was significantly higher than that in the left hemisphere, showing more distribution of Lf-PO-Dox/Tet in the right hemisphere where the glioma was located, which indicated that Lf-PO-Dox/Tet was able to enter the brain and further concentrate at the tumor site.

Dox distribution in other tissues showed that polymersomes accumulated most in the spleen with the liver ranking next (Figure 10). Concentration of Lf-PO-Dox/Tet and Lf-PO-Dox in spleen was significantly lower than that of PO-Dox/Tet and PO-Dox respectively, indicating that Lf conjugation reduced the accumulation of polymersomes in spleen, which was in accordance with the literature.[8] There was no significant difference of drug distribution in other major organs such as kidney, heart, and lung between groups. Polymersomes of the four groups presented a relatively low accumulation in the heart, suggesting that polymersome Dox might have similar potential as liposome Dox to decrease heart toxicity of Dox.

Pharmacodynamics Experiments in Glioma Model Rats. As shown in Figure 11, the Lf-PO-Dox/Tet group presented the smallest glioma volume for rats sacrificed on the same day. Especially for rats sacrificed on the 14th day, the tumor volume of the Lf-PO-Dox/Tet group was significantly lower than those of the other four groups, indicating Lf-PO-Dox/Tet treatment effectively inhibited the rapid growth of glioma.

Life-span extension treated with a multidose of 1.5 mg/kg Dox on days 2, 5, 8, and 11 after glioma implantation exhibited diversity with different formulations (Figure 12). By log-rank test (Table 2), the median survival times of four polymersome groups except the PO-Dox group were all significantly prolonged compared with that of saline control. However, the increase in survival times (IST) of the Lf-PO-Dox/Tet group was more considerable when compared with any other group except Lf-PO-Dox group ($p < 0.05$), which reached nearly 82% and 63% life-span extension compared with the saline control and PO-Dox group. As compared with the Lf-PO-Dox group, the Lf-PO-Dox/Tet group showed

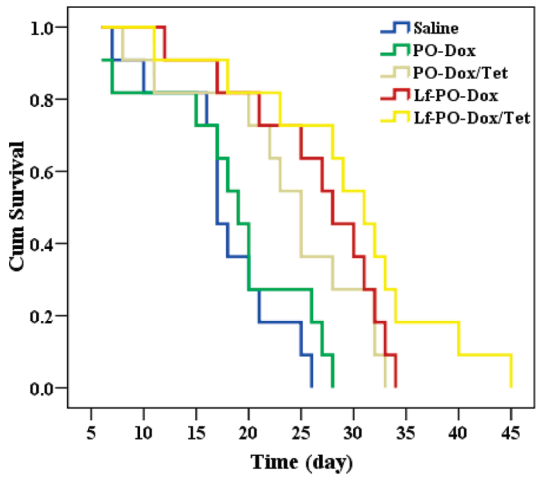

Figure 12. Percentage of survival (Kaplan−Meier plot) of glioma bearing rats after intravenous injection of 1.5 mg/kg Dox on days 2, 5, 8, and 11 with different formulations ($n = 11$).

higher median survival time but with no significance. Significant life-span extension was observed for the Lf-PO-Dox group, and PO-Dox/Tet vs PO-Dox confirmed that both Lf and Tet enhanced the antitumor effect of Dox loaded polymersomes.

Discussion

Chemical and physical properties of the nanoparticles, including size, surface charge, and surface chemistry, are important factors that determine their pharmacokinetics (PK) and biodistribution, which largely define their therapeutic effect and toxicity.[31] Maintaining the size around 100 nm is most optional for improving the PK of nanoparticles[31] and advantageous for endocytosis by brain capillary endothelial cells.[32] In fact, vesicle size of polymersomes in this study was around 220 nm, which might attribute to high distribution of polymersomes in spleen and liver where the mononuclear phagocyte system (MPS) mainly was located. However, one of the features of glioma is neoangiogenesis with newly formed vessels generally not displaying BBB properties that are characteristic for normal brain vasculature,[33] leading to high vascular density in solid brain tumors, large gaps between endothelial cells in tumor blood vessels, and the emerging of EPR effects at advanced stage of solid brain tumor.[34] The frequency distribution histogram of brain tumor endothelial gap size has a modal value of 0.38 μm.[35] Moreover, glioma has the ability to actively degrade tight junctions by secreting soluble factors, eventually leading to BBB disruption within invaded brain tissues.[36] Therefore, in the condition of glioma, a leaky brain vasculature facilitated the bypassing of drug delivery systems even with vesicle size beyond 200 nm like the polymersomes in this study, which was verified by weak distribution of DiR labled polymersomes at the glioma site.

The MRT_{0-t} of all groups of polymersomes ranged from 21 to 28 h, showing longer plasma circulation time than PEGylated nanoparticles by several-fold,[37] as comparable to PEG-based liposomal systems,[28,38] which might be due to the relative neutral zeta potential and full PEGylation on the surface of polymersomes. In this study, the zeta potential of all groups of polymersomes ranged from −10 to −9 mV, which agreed well with the optional zeta potential within 10 mV, and might be helpful to decrease MPS uptake and prolong blood circulation compared to the charged ones.[31] Surface modification with poly(ethylene glycol) reduces the rate of MPS uptake and prolongs the circulation half-life of nanoparticles. Long circulation of nondegradable polymersomes has already been found to increase with increasing PEG chain length.[23] The surface PEG of biodegradable polymersomes in this study had long PEG chains of 3000 Da which might impart perfect stealth in blood. Moreover, the full hydrophilic PEG (100%) content than PEGylated liposome (5%−10% PEGylation) should confer better resistance to opsonization and thereby extend vesicle circulation times.[18]

According to the theory on pharmacokinetics of brain drug delivery put forward by Pardridge, the amount of drug that entered the brain was positively correlated with permeability coefficient surface area product (PS) of the drug against the brain tissue and AUC of the drug in the blood.[39] Therefore, increased brain drug delivery could be achieved by prolonging systemic circulation of the drug (namely, increasing AUC) and meanwhile improving the permeability of the drug against brain tissue. The polymersome constructed in this study was expected to be granted an elevated permeability

(31) Li, S. D.; Huang, L. Pharmacokinetics and biodistribution of nanoparticles. *Mol. Pharmaceutics* **2008**, *5* (4), 496–504.
(32) Huwyler, J.; Wu, D.; Pardridge, W. M. Brain drug delivery of small molecules using immunoliposomes. *Proc. Natl. Acad. Sci. U.S.A.* **1996**, *93* (24), 14164–14169.
(33) Kemper, E. M.; Boogerd, W.; Thuis, I.; Beijnen, J. H.; Tellingen, O. V. Modulation of the blood-brain barrier in oncology: therapeutic opportunities for the treatment of brain tumours. *Cancer Treat. Rev.* **2004**, *30*, 415–423.
(34) Fang J. ; Nakamura H. ; Maeda H. The EPR effect: Unique features of tumor blood vessels for drug delivery, factors involved, and limitations and augmentation of the effect. *Adv. Drug Delivery Rev.* **2010**. DOI: 10.1016/j.addr.2010.04.009.
(35) Schlageter, K. E.; Molnar, P.; Lapin, G. D.; Groothuis, D. R. Microvessel organization and structure in experimental brain tumors: microvessel populations with distinctive structural and functional properties. *Microvasc. Res.* **1999**, *58* (3), 312–28.
(36) Schneider, S. W.; Ludwig, T.; Tatenhorst, L.; Braune, S.; Oberleithner, H.; Senner, V.; Paulus, W. Glioblastoma cells release factors that disrupt blood-brain barrier features. *Acta Neuropathol.* **2004**, *107*, 272–276.
(37) Lu, W.; Wan, J.; She, Z.; Jiang, X. G. Brain delivery property and accelerated blood clearance of cationic albumin conjugated pegylated nanoparticle. *J. Controlled Release* **2007**, *118* (1), 38–53.
(38) Cui, J.; Li, C.; Guo, W.; Li, Y.; Wang, C.; Zhang, L.; Zhang, L.; Hao, Y.; Wang, Y. Direct comparison of two pegylated liposomal doxorubicin formulations: is AUC predictive for toxicity and efficacy. *J. Controlled Release* **2007**, *118* (2), 204–15.
(39) Pardridge, W. M. *Brain drug targeting*; Cambridge University Press: Cambridge, 1998; p 82.

Table 2. Median Survival Time for Glioma Implanted Rats of Different Therapeutic Groups[a]

group	median (day)	standard error	95% confidence interval	log-rank test	ISTC (%)	ISTG (%)
Saline	17.0	0.8	15.4−18.6			
PO-Dox	19.0	1.2	16.6−21.4		12	
PO-Dox/Tet	25.0	1.6	21.9−28.1	[b,c]	47	32
Lf-PO-Dox	28.0	2.8	22.6−33.4	[b,c]	65	47
Lf-PO-Dox/Tet	31.0	2.2	26.7−35.3	[b,c,d]	82	63

[a] Dosage of Dox is 4 ×1.5 mg/kg. Log-rank test vs control. [b] $p < 0.01$ vs saline. [c] $p < 0.01$ vs PO-Dox. [d] $p < 0.05$ vs PO-Dox/Tet. The increases in survival times (%) are compared to saline control (ISTC) or to PO-Dox group (ISTG).

to brain tumor tissues through Lf conjugation and be armed with long circulation property through full PEGylation and neutral zeta potential. Pharmacokinetic parameters showed that AUC_{0-t} of Lf-PO-Dox/Tet and Lf-PO-Dox was lower than that of PO-Dox/Tet and PO-Dox, respectively, which might result from the increased uptake by MPS and distribution to organs such as liver after Lf conjugation, resulting in rapid decline in plasma concentration in the first 10 min after drug administration. However, Lf conjugation did not influence the long circulation property of polymersomes significantly in this study. In vivo imaging showed that Dir labeled Lf-PO could concentrate in the brain tumor, significantly more effective than unmodified polymersomes, indicating intensified permeability of polymersomes to the brain tumor by Lf decoration. The intensified permeability of polymersomes was also verified by higher distribution of Lf-PO-Dox/Tet than PO-Dox/Tet at the glioma site. Therefore, with both unchanged long circulation property and enhanced capability in drug delivery to the brain tumor, Lf-PO-Dox/Tet's therapeutic effect could be expected. In fact, in pharmcodynamic evaluation, model rats treated with Lf-PO-Dox/Tet presented significantly smaller tumor volume and longer median survival time than rats treated with PO-Dox/Tet, indicating effective inhibition of tumor growth, which was in good accordance with the pharmacokinetic results.

A targeting ligand conjugated to the surface of nanoparticles can recognize and bind with the receptor expressed on the target cell surface, which later triggers receptor-mediated endocytosis, resulting in an increased level of intracellular delivery of the formulation.[31] The quantitative determination revealed that C6 cell uptake of Lf-PO-Dox/Tet and Lf-PO-Dox increased with time, and was significantly higher than that of PO-Dox/Tet and PO-Dox, repectively, indicating that Lf decoration enhanced the intracellular delivery rate of the drug loaded vesicle. Moreover, further in vitro cytotoxicity confirmed Lf conjugation granted Dox-loaded vesicle stronger inhibition capability that made it exert its cytotoxicity toward C6 cells at a significantly lower concentration, which was in accordance with the cell uptake results. Considering LRP, the receptor of Lf, was overexpressed by glioma cells, especially in cell lines of human origin such as U87 and SF-539,[11] and C6 cells[12] of rat origin, Lf conjugation might facilitate the tumor cell uptake of polymersomes via LRP-mediated endocytosis as it did with nanoparticles.[9,13]Therefore, increasing the rate of intracellular delivery to glioma cells by conjugating Lf on the surface of polymersomes might be the main cause for enhanced permeability of Lf-conjugated polymersomes to brain tumor. Further study on the uptake mechanism employing immunofluorescence technique and inhibition experiments is undergoing at present to verify this point.

The capability of Lf-conjugated polymersomes across the BBB might also contribute to enhanced permeability to the brain tumor. For the chemotherapy of the active glioma cells of brain parenchymal metastases, the ability of Lf-conjugated polymersomes to penetrate the BBB is critical to prevent the active glioma cells from further invasion into normal brain parenchyma. In this study, both in vivo imaging and tissue distribution indicated that Lf conjugation could increase the brain uptake of polymersomes, which agreed well with our previous reports that surface Lf decoration could increase the brain delivery of nanoparticles.[9]

Tet also played an important role in the enhanced permeability of polymersomes to the brain tumor. PO-Dox/Tet and Lf-PO-Dox/Tet exhibited much higher cell uptake than PO-Dox and Lf-PO-Dox, respectively, indicating that Tet enhanced the tumor cell uptake of the drug loaded vesicle. Further MTT assay revealed that the IC_{50} of PO-Dox was 32.2 μg/mL, about 1.7 times that of PO-Dox/Tet, meaning that the Tet-loaded vesicle had an intensified cytotoxicity toward C6 cells, which conformed well to the cell uptake results. Tissue distribution and pharmacodynamics also revealed that Tet increased glioma drug delivery and extended the survival of glioma bearing rats. As a potent MDR inhibitor, Tet could reverse MDR of MCF/adr cells toward Dox both in vivo and in vitro[22] and increase the accumulation in K562/A02 cells of Dox encapsulated in magnetic nanoparticles;[40] however, the action mechanism of Tet was not clear. It was proved that Tet could down-regulate the transcriptional level of mdr1 (the gene sequence coding P-gp), while the existing expression of P-gp was not affected.[41] This means that, in the repeated or long-term drug administration to tumor cells, Tet could prevent the generation of MDR. However, this point could not be used to explain the results in our study, because, different from the above-mentioned MCF/adr and K562/A02 cell lines, the C6

(40) Chen, B. A.; Sun, Q.; Wang, X. M. Reversal in multidrug resistance by magnetic nanoparticle of Fe_3O_4 loaded with adriamycin and tetrandrine in K562/A02 leukemic cells. *Int. J. Nanomed.* **2008**, *3* (2), 277–286.

(41) Shen, H. L.; Xu, W. L.; Chen, Q. Y. Tetrandrine prevents acquired drug resistance of K562 cells through inhibition of mdr1 gene transcription. *J. Cancer Res. Clin. Oncol.* **2010**, *136*, 659–665.

cell line cultured in this study was not drug resistant. The exclusive reasonable explanation might be that Tet functionally inhibited P-gp or other drug-resistant factors overexpressed in glioma cells and its blood vessels, and at the BBB by decreasing the fluidity of the cell membrane and possibly affecting the ATP enzymatic activity of P-gp, resulting in the inhibition of exocytosis,[22] which was still in need of further verification.

Conclusions

Lf-conjugated polymersomes constructed in this study were proved to have the ability to target glioma by in vivo imaging of brain fluorescence. After loading of Dox and Tet, the obtained Lf-PO-Dox/Tet displayed higher cell uptake and stronger inhibition toward C6 cells and more accumulation in the brain tumor site, which was in good accordance with its better therapeutic efficacy of glioma model rats manifested by more effective inhibition of glioma growth and prolonged median survival time. Taken together, Lf-PO-Dox/Tet is a prospective drug delivery system for targeting therapy of gliomas.

Acknowledgment. This work was supported by the National Basic Research Program of China (973 Program, 2007CB935802), the National Key Program of Pharmaceutical Creation and Development (2009ZX09310-006), and the young teacher's initiative foundation of School of Pharmacy, Fudan University.

MP100277H